Time correlation functions of simple liquids: a new insight on the underlying dynamical processes.

Giovanni Garberoglio[1], Renzo Vallauri[2,3] and Ubaldo Bafile[3]

[1]European Centre for Theoretical Studies in Nuclear Physics and Related Areas (ECT*-FBK), Strada delle Tabarelle 286, I-38123 Villazzano (TN), Italy and Trento Institute for Fundamental Physics and Applications (TIFPA-INFN), via Sommarive 18, I-38123, Povo (TN), Italy
[2]Consiglio Nazionale delle Ricerche, Istituto dei Sistemi Complessi, via Madonna del Piano, I-50019 Sesto Fiorentino, (FI), Italy
[3]Consiglio Nazionale delle Ricerche, Istituto Fisica Applicata "Nello Carrara", via Madonna del Piano, I-50019 Sesto Fiorentino, (FI), Italy

Abstract

Extensive molecular dynamics simulations of liquid sodium have been carried out to evaluate correlation functions of several dynamical quantities. We report the results of a novel analysis of the longitudinal and transverse correlation functions obtained by evaluating directly their self and distinct contributions at different wavevectors k. It is easily recognized that the self-contribution remains close to its $k \to 0$ limit, which turns out to be exactly the autocorrelation function of the single particle velocity. The wavevector dependence of the longitudinal and transverse spectra and their self and distinct parts is also presented. By making use of the decomposition of the velocity autocorrelation spectrum in terms of longitudinal and transverse parts, our analysis is able to recognize the effect of different dynamical processes in different frequency ranges.

1. Introduction.

In recent years, the study of dynamical properties of simple monoatomic liquids has received a strong impetus, due to the massive use of new experimental techniques. The large use of X ray [1] and neutron sources [2] along with advanced spectroscopic facilities have allowed the observation of dynamical processes occurring in the terahertz frequency range with surprising good accuracy. Since the seminal works on liquid alkali metals [3], attention has been devoted to other

liquid metals [4], often supplemented by molecular dynamics evaluation of the relevant quantities. The accurate experimental data have initially been exploited to derive the physical parameters necessary to reproduce the experimental spectra in the generalized hydrodynamic framework [3]. In fact, these systems have generally been regarded as "simple" liquids and consequently their theoretical description was carried out according to the same lines used at early stages for an analytical interpretation of the experimental and molecular dynamics results [5]. On the other hand, the detailed experimental lineshapes suggested the possibility of discerning the influence of dynamical effects other than those traditionally considered in the explanation of the so-called Rayleigh-Brillouin region. The underlying idea is that in the terahertz frequency region where the wavelength becomes close to the atomic nearest neighbor distance, a solid-like cage effect acts as a restoring force for transverse acoustic modes, which eventually can give a contribution to the dynamical structure factor $S(k, \omega)$. Therefore in most of the papers dealing with liquid metals [4] a search for the appearance of transverse contributions was accomplished both in $S(k, \omega)$ and in the longitudinal current $C_L(k, \omega)$. Particularly interesting are the results of liquid sodium obtained by Giordano and Monaco [6]. They showed that liquid sodium exhibits acoustic excitations of both longitudinal and transverse polarization at frequencies very close to those of the polycrystal, the only difference being restricted to line broadening. Molecular dynamics [MD] computations of the longitudinal and transverse current correlation functions at different wavevectors and their relative spectra showed a good agreement between experimental and MD peak frequencies [7].

In the present paper, we present molecular dynamics calculations of the longitudinal and transverse currents and the separate contributions of their respective self and distinct terms. In discussing the corresponding spectra, we believe that a clear picture of the dynamical processes responsible for their behavior will emerge. In particular, our analysis will highlight the connection between collective propagation excitations (both longitudinal and transverse) beyond the hydrodynamic limit and single particle dynamical processes with long and short time scales.

We have performed the calculations for all the alkali metals but, for the sake of brevity, we report here only the results for liquid sodium, since no major differences are found to occur apart from a time scaling as suggested in a previous paper [8]

2. Dynamical quantities of interest and simulation procedures.

Let us start defining the quantities of interest in our investigation. According to the usual notation, we start considering the *current* associated with the motion of *N* particles:

$$j(\mathbf{k}, t) = \sum_i \mathbf{v}_i(t) \exp(i\mathbf{k} \cdot \mathbf{r}_i(t)) \tag{1}$$

and define the normalized *longitudinal* and *transverse* current correlation functions:

$$C_L(k,t) = \frac{\langle j_z(k,t) j_z^*(k,0)\rangle}{\langle j_z(k,0) j_z^*(k,0)\rangle} = \frac{\langle \sum_{i,j} v_j^z(t) v_i^z(0) e^{ik(z_j(t)-z_i(0))}\rangle}{\langle \sum_i v_i^z(0) v_i^z(0)\rangle} \tag{2}$$

$$C_T(k,t) = \frac{\langle j_x(k,t) j_x^*(k,0)\rangle}{\langle j_x(k,0) j_x^*(k,0)\rangle} = \frac{\langle \sum_{i,j} v_j^x(t) v_i^x(0) e^{ik(z_j(t)-z_i(0))}\rangle}{\langle \sum_i v_i^x(0) v_i^x(0)\rangle} \tag{3}$$

having chosen the vector $\mathbf{k}$ along the z-direction. With obvious notations $v_i^z(t)$ represents the z-component of the velocity of the *i-th* particle at time *t*, and $z_i(t)$ the z-component of its position. The brackets $\langle ... \rangle$ indicate a statistical average. We then evaluate the *self-part* of (2) and (3) by setting *i=j* in the double sums. They read:

$$C_L^{self}(k,t) = \frac{\langle \sum_i v_i^z(t) v_i^z(0) e^{ik(z_i(t)-z_i(0))}\rangle}{\langle \sum_i v_i^z(0) v_i^z(0)\rangle} \tag{4}$$

$$C_T^{self}(k,t) = \frac{\langle \sum_i v_i^x(t) v_i^x(0) e^{ik(z_i(t)-z_i(0))}\rangle}{\langle \sum_i v_i^x(0) v_i^x(0)\rangle} \tag{5}$$

3

so that:

$$C_L(k,t) = C_L^{self}(k,t) + \frac{\langle \sum_{i \neq j} v_j^z(t) v_i^z(0) e^{ik\left(z_j(t) - z_i(0)\right)} \rangle}{\langle \sum_i v_i^z(0) v_i^z(0) \rangle} =$$

$$= C_L^{self}(k,t) + C_L^{distinct}(k,t) \tag{6}$$

$$C_T(k,t) = C_T^{self}(k,t) + \frac{\langle \sum_{i \neq j} v_j^x(t) v_i^x(0) e^{ik\left(z_j(t) - z_i(0)\right)} \rangle}{\langle \sum_i v_i^x(0) v_i^x(0) \rangle} =$$

$$= C_T^{self}(k,t) + C_T^{distinct}(k,t) \tag{7}$$

We obtain the *distinct-part* by subtraction of the *self-part* from the *total* that will be referred to as *full* in the following. An important observation is in order. At $t = 0$ the *distinct-part* turns out to be zero since it contains the statistical average of velocity components of different particles. As a consequence, the integral of its Fourier spectrum is zero and therefore must comprehend positive and negative contributions. Needless to say, it represents a quantity which cannot be derived by any direct experiment.

In the subsequent discussions, a crucial role will be played by the normalized single particle velocity auto-correlation function:

$$\psi(t) = \frac{\langle \sum_i \boldsymbol{v}_i(t) \cdot \boldsymbol{v}_i(0) \rangle}{\langle \sum_i \boldsymbol{v}_i(0) \cdot \boldsymbol{v}_i(0) \rangle} \tag{8}$$

as well as by the self-intermediate scattering function:

$$F_S(k,t) = \frac{1}{N} \langle \sum_i e^{ik\left(z_i(t) - z_i(0)\right)} \rangle \tag{9}$$

4

Molecular dynamics runs were carried out on liquid metals by using the classical potential model implemented by Price et al. [9]. We used a cubic box containing 512 sodium atoms, with a side length of 27.63 Å corresponding to a density of 927 kg/m^3. The simulation was performed by an in-house developed code at a temperature of T=395 °K, fixed using a Berendsen thermostat with a coupling constant τ=1 ps. The system was equilibrated for 500 ps, after which we performed a production run of 2 ns, saving the trajectories for offline analysis by means of another in-house developed code. The timestep used was 2 fs.

3. Results and discussion.

In figure 1 we report the results of the longitudinal and transverse correlation functions and their components at the wavevector k= 0.394 Å^{-1}. This is not the minimum wavevector accessible in our simulation, but it has been chosen because the transverse current shows clear oscillations indicating that shear modes are supported. We wish to point out that for all the wavevectors examined the dynamical structure factor shows a well-defined peak indicating that longitudinal waves are supported, as experimentally confirmed [3].

Firstly, we observe that the *self-part* is very similar in both longitudinal and transverse correlation functions. In fact, an inspection to equations (6) and (7) suggests the cause. The self-contributions turn out to contain the correlation of the single particle velocity multiplied by the exponential of the displacement of the same particle i. If the time scale over which the velocity correlation of a single particle decays to zero is much shorter than the diffusion time, the factorization of the terms containing the velocity and the coordinate variables can be applied. As a consequence, the *self-part* of longitudinal and transverse correlation functions can be written as the product of the velocity auto-correlation function times the self-intermediate scattering function. Since at the wavevector k= 0.394 Å^{-1}, $F_S(k,t)$ changes very little during the time over which $\psi(t)$ decays to zero, the self-contribution of both the longitudinal and transverse correlation functions is

almost identical to the velocity auto-correlation function. This result will be exploited in the description of the corresponding spectra.
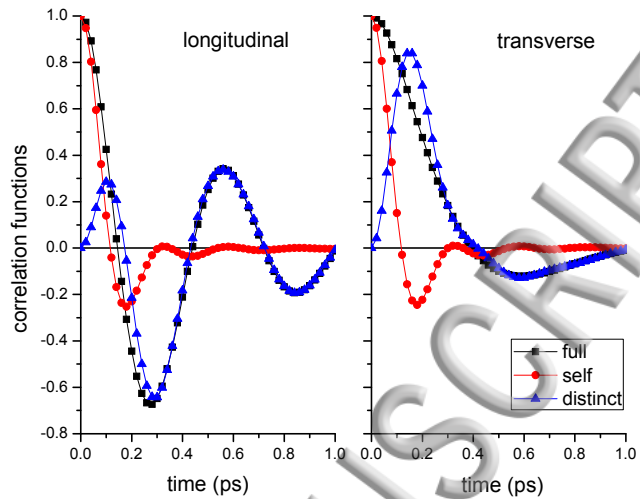

Figure 1.

Longitudinal and transverse correlation functions along with their self and distinct contributions. $k = 0.394$ Å^{-1}

A quantitative measurement of such deviations is shown in figure 2. The difference does not exceed 1% and as is evident, the larger deviation is achieved by the longitudinal *self-term*, a characteristic that will be discussed later in combination with the evolution of the *distinct-part* at different wavevectors.
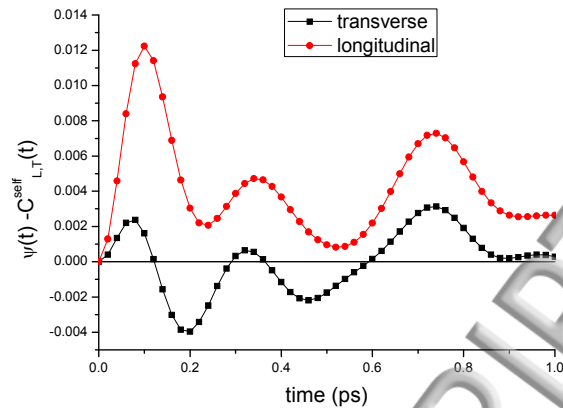
Figure 2.

Difference between the velocity auto-correlation function and the self-part of the longitudinal (points) and transverse (squares) correlation functions. $k = 0.394$ Å^{-1}

Let us now discuss the behavior of the *distinct-part*. It contains the correlation of the velocity of different particles, i.e. it is a measure of how the velocity, let's say of particle 1, is transferred to particle 2. This effect is mostly evident in the case of the transverse correlation. In fact, the *distinct-term* increases from zero to its maximum value at the time when the velocity of particle 1 has reached its minimum (see figure 1). Such a behavior is the evidence of what has been referred to as "momentum transfer". A thorough analysis of this effect in Lennard-Jones fluids has been carried out by Balucani et al. [10], who stressed the importance of understanding the cooperative effects amongst nearest and next-nearest neighbors for better understand single-particle motion. The correlation established by the presence of the term $e^{ik\left(z_j(t) - z_i(0)\right)}$ gives rise to the subsequent oscillations. The same effect is present in the longitudinal current even if it appears that the transfer of momentum is less complete since the correlation induced by the exponential term considerably reduces its influence. The presence of different components for the velocity (*x-*

component) and the position (*z*-component) in the transverse current, contrasted with the situation of the longitudinal current (*z*-component for the velocity as well as for the position) can be the reason for this different behavior.

A great deal of basic information can be derived from the inspection of the longitudinal and transverse spectra and their components, shown in figures 3 and 4 respectively. For the sake of clarity, we call "full" the spectrum of the total correlation function, either longitudinal or transverse, and "self" the Fourier transform of what we call *self-term* of the currents; as already mentioned, "distinct" is the difference between "full" and "self".
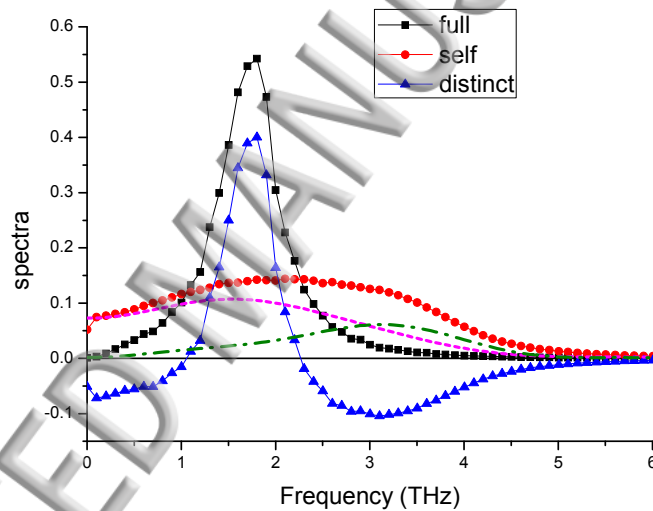

Figure 3

Longitudinal current spectrum (full) along with

its components (self and distinct) at $k = 0.394$ Å^{-1}.

The longitudinal and transverse contributions to

the self-term, obtained from $\psi(\omega)$, are shown,

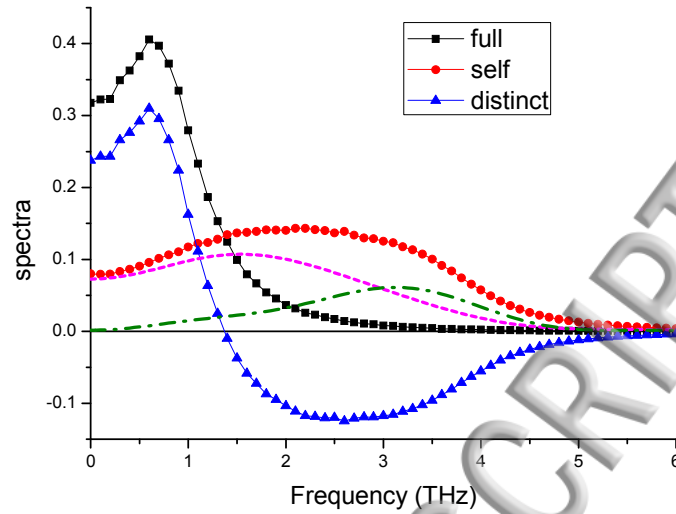dash-dotted (green) and dotted lines (pink)

respectively.

8

Figure 4

Transverse current spectrum (full) along with its

components (self and distinct) at k = 0.394 Å^{-1}.

The longitudinal and transverse contributions to

the self-term, obtained from $\psi(\omega)$, are shown,

dash-dotted (green) and dotted lines(pink)

respectively.

As is evident, the distinct part of the spectra contains a negative contribution and therefore, it is not a physical quantity directly measurable by any real experiment. Nevertheless, the behavior in different regions of the spectrum gives important indications on the underlying physical processes, i.e. those involved in the single particle dynamics as well as those explicitly dependent on two particle correlations. The negative intensities in the spectra highlight the effect of these last terms. For example, the position of the well-defined peak in the longitudinal spectrum is a consequence of the fact that both at frequencies lower and higher than the frequency maximum there is a large subtraction of the intensity coming from the self-contribution, by the distinct

9

contribution. In the transverse spectrum, there is a large cancellation of intensity at frequencies larger than the maximum. In both cases, however, the intensity of the peak is the sum of self and distinct contributions.

Let us firstly examine the *self-part* of the longitudinal spectrum. As already pointed out the *self-part* of the longitudinal current is close to the velocity correlation function. Indeed, it is easily recognized that the self-part of the longitudinal current correlation function turns out to be:

$$C_L^{self}(k,t) = \frac{1}{A}\left[-\frac{1}{k^2}\frac{d^2 F_S(k,t)}{dt^2}\right] \tag{10}$$

with $A = \langle \sum_i v_i^z(0)v_i^z(0)\rangle$ and consequently the *self-part* of the spectrum reads:

$$C_L^{self}(k,\omega) = \frac{1}{A}\left[-\frac{\omega^2}{k^2}S_S(k,\omega)\right] \tag{11}$$

As $k \to 0$, the self-spectrum coincides with the spectrum $\psi(\omega)$ of the normalized velocity auto-correlation function and at larger k it starts to deviate from $\psi(\omega)$. At the present wavevector $k=$ 0.394 Å^{-1}, we notice that, apart the region around $\omega = 0$ where the self-spectrum gets close to zero, $C_L^{self}(k,\omega)$ is found to be almost coincident with $\psi(\omega)$, which is not reported in the figures.

In the transverse spectrum, as pointed out in figure 4, this situation is even more marked; in fact, there is no analogue of equation (10) because different components of velocity and position are involved in the transverse current correlation function.

This circumstance allows us a new and somehow deeper reading of the current spectra and possibly a better understanding of the underlying physical processes. To this aim, we resort to the representation of the $\psi(t)$ in terms of longitudinal and transverse currents introduced by Gaskell and Miller [11], i.e.

10

$$\psi(t) \approx \frac{1}{(2\pi)^3} \int d\boldsymbol{k} \, f(k)[C_L(k,t) + 2C_T(k,t)] \, F_S(k,t) \tag{12}$$

Where $f(k)$ is the Fourier transform of the quantity $f(r)$ that characterizes the microscopic velocity field. If the form factor $f(r)$ is chosen to be constant across a suitable length scale a (of the order of interparticle separation), $f(k)$ is given by:

$$f(k) = \frac{3}{n} \frac{j_1(ka)}{ka} \tag{13}$$

where $j_1(ka)$ is the spherical Bessel function of order one and n the number density. If one neglects the time dependence of $F_S(k,t)$, $\psi(\omega)$ turns out to be written as:

$$\psi(\omega) \approx \frac{2}{3\pi} \int_0^\infty \frac{j_1(ka)}{ka} [C_L(k,\omega) + 2C_T(k,\omega)] \, k^2 \, dk = \psi_L(\omega) + \psi_T(\omega) \tag{14}$$

with obvious definition of the quantities $\psi_L(\omega)$ and $\psi_T(\omega)$. By using our computer simulation results for the current correlation functions and their relative spectra, we are able to perform the integral in equation (14) and find the longitudinal ($\psi_L(\omega)$) and transverse ($\psi_T(\omega)$) contributions of the spectrum of the normalized velocity autocorrelation function. In view of the fact that such spectrum is very near to the self-part $C_L^{self}(k,\omega)$ we are able to distinguish the role of these two components to the full spectrum. The results are reported in figures 3 and 4, where the longitudinal and transverse contributions are shown as dash-dotted and dotted lines, respectively.

Let us start by examining the longitudinal spectrum (figure 3). In the low frequency range (0 < ω < 1 THz), the *self-part* of the spectrum is mostly due to the transverse component $\psi_T(\omega)$, which is strongly depleted, in the full spectrum, by physical processes which rule the distinct part. In the frequency range between 1 and 2.5 THz, both contributions of self and distinct parts are

11

equally significant and give rise to a well-defined peak. At $\omega > 2.5$ THz, where the transverse and longitudinal contributions to the spectrum of the *self-part* are about the same, there is again a strong cancellation that determines the rapid decrease of the longitudinal spectrum.

The interpretation of the transverse spectrum is even simpler since the peak at $\omega \approx 1$ THz is due to the sum of contributions from the *self-part* (where the transverse component $\psi_T(\omega)$ is predominant) and from processes responsible for the distinct term. At larger frequencies, the cancellation due to the distinct part dominates and the spectrum goes rapidly to zero.

Let us now consider larger wavevectors. In figures 5, 6 and 7 we present the results for the longitudinal and transverse current correlation functions and the relative spectra at $k = 0.643$ Å^{-1} respectively.
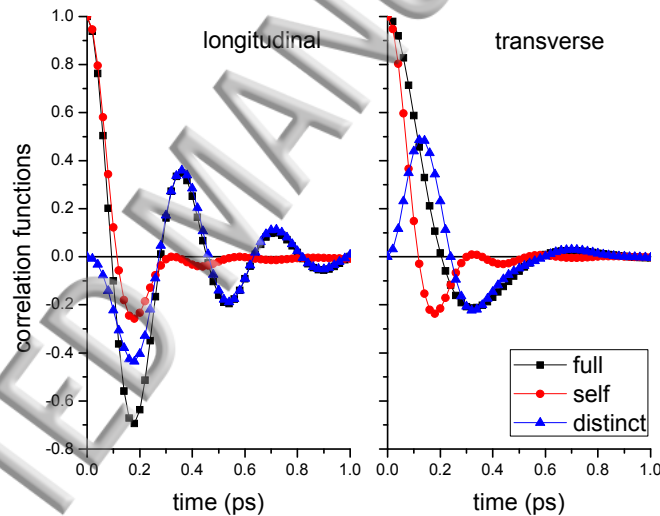

Figure 5.

Longitudinal and transverse correlation

functions along with their self and

distinct contributions. $k = 0.643$ Å^{-1}

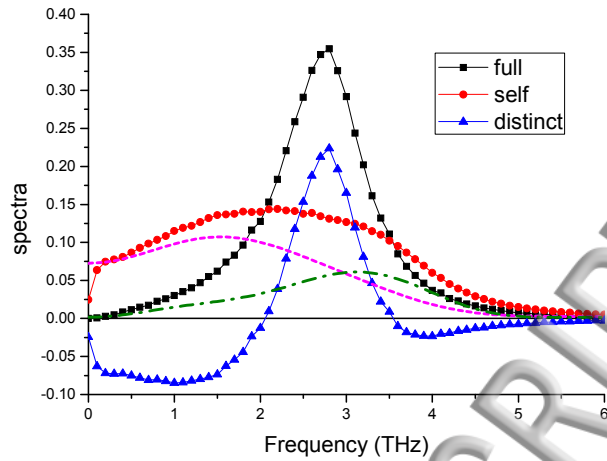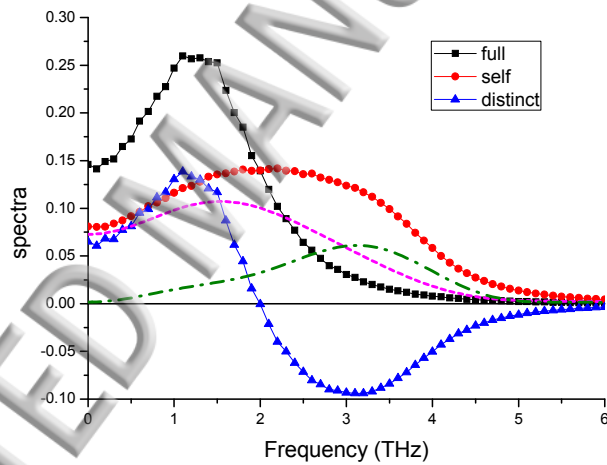Figure 6

Same as figure 3 at k= 0.643 Å^{-1}

Figure 7

Same as figure 4 at k= 0.643 Å^{-1}

The most noticeable difference with respect to the previous wavevector is the initial behavior of the distinct part for the longitudinal current. In fact, it decreases becoming negative at short times, contrary to what happens at the smaller wavevector previously examined, and to the transverse distinct term in the present case.

13

As far as the spectra are concerned, an inspection to figure 6 confirms the large subtraction of intensity in the range between 0 and 2 THz in the longitudinal spectrum where the relevant contribution comes from the transverse component $\psi_T(\omega)$ of the self-spectrum. Considering the transverse spectrum, we notice that both the self and distinct parts contribute to the peak at 1 THz, whereas these two components have opposite signs in the region between 2 and 4 THz, resulting in cancellation.

The last wavevector examined is $k= 1.287$ Å^{-1} and the relative correlation functions and spectra are reported in figures 9, 10 and 11 respectively. Whereas the distinct part of the longitudinal current becomes still negative at short times, the distinct component of transverse current is now very close to zero.
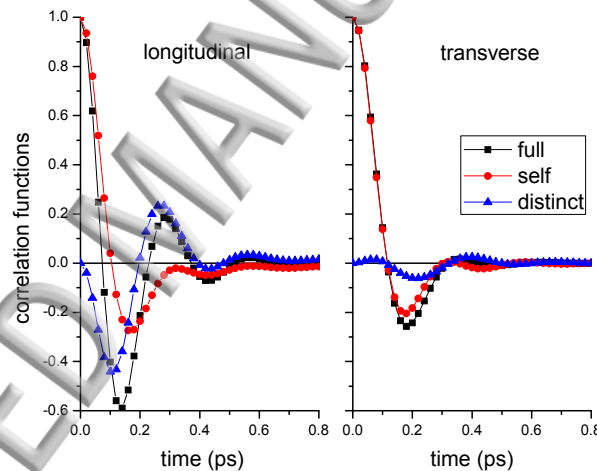

Figure 8.

Longitudinal and transverse correlation functions along with their self and distinct contributions. $k= 1.287$ Å^{-1}

The longitudinal spectrum shows an even more marked cancellation of the self-contribution in the range $0<\omega<2$ THz. It is worthwhile to point out that at the present wavevector, which

corresponds to a wavelength $\lambda = 2\pi/k = 4.88\,\text{Å}$ the dynamical structure factor presents still a well-defined peak, indicating that the system can always support longitudinal waves.
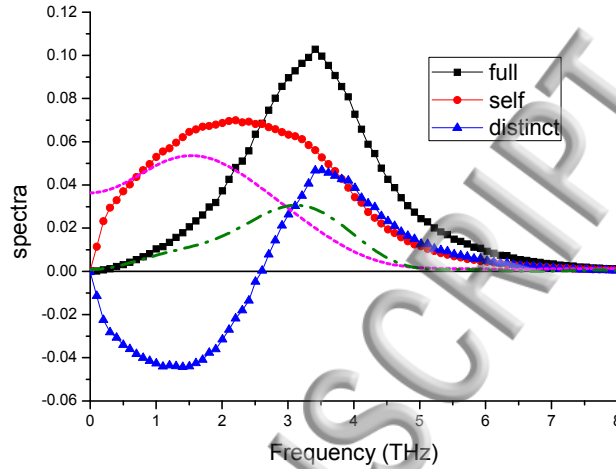

Figure 9

Same as figure 4 at k= 1.287 Å^{-1}

The transverse spectrum, reported in figure 11, reveals that shear waves present at this wavelength reflect mostly the dynamical processes present in the *self-part*, being the distinct contribution in the range of the peak around 2.5 THz very feeble.
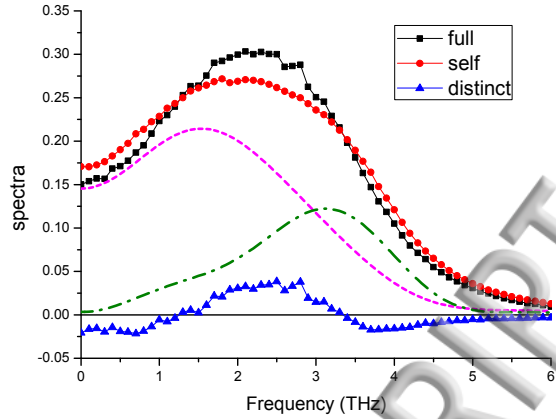
Figure 10

Same as figure 4 at $k = 1.287$ Å^{-1}

The initial onset of the correlation functions can easily be inspected by evaluating the normalized second frequency moments of the self and distinct contributions to the longitudinal and transverse currents. Such a task has been tackled since the early study of simple monatomic liquids, with the aim of supplying a realistic interpretation of the dynamical structure factor [12] via the Mori-Zwanzig [13] theory of many body problems. The separate contributions of the *self* and *distinct* parts for the longitudinal currents, read:

$$\omega^2_{L,self} = \frac{3k_B T}{m} k^2 + \omega^2_E \tag{14 a}$$

$$\omega^2_{L,distinct} = -\omega^2_E \big(j_0(kr_0) - 2j_2(kr_0) \big) \tag{14 b}$$

and for the transverse currents:

$$\omega^2_{T,self} = \frac{k_B T}{m} k^2 + \omega^2_E \tag{15 a}$$

$$\omega^2_{T,distinct} = -\omega^2_E \big(j_0(kr_0) + j_2(kr_0) \big) \tag{15 b}$$

16

where k_B indicates the Boltzmann constant, T the temperature, m the mass and ω_E the Einstein frequency. $j_0(kr_0); j_2(kr_0)$ are the spherical Bessel functions of order 0 and 2, where r_0 is close to the core diameter and can be taken equal to the parameter a introduced in equation 13. A deeper discussion of the approximations leading to expressions (14 a,b) and (15 a,b) can be found in references [3,10,11]. We are able to evaluate separately $\omega^2_{L,distinct}$ and $\omega^2_{T,distinct}$ using the value of ω^2_E derived from $\psi(t)$; the resulting quantities changed of sign provide the values of the second time derivatives of the proper correlation functions. Figure 11 shows these results.
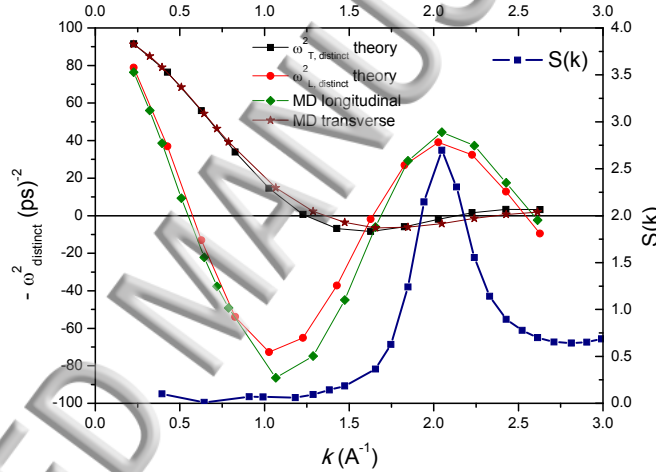

Figure 11.

The second moment (changed of sign) of the distinct contributions to the longitudinal and transverse currents evaluated from equations (14b) and (15b) and obtained directly from the molecular dynamics results. For convenience we present also the structure factor $S(k)$.

It is worth stressing that according to the mentioned correspondence between second time derivative and second moment, a negative $-\omega_{L,T,distinct}^2$ implies that the corresponding *distinct* current correlation functions initially decay from their zero time value. The agreement between molecular dynamics data and theory is excellent. Gaskell and Duffy [14], who gave an estimate of the distinct contribution to the transverse correlation function by using the velocity field approach [11] along with the Vineyard approximation to carry on the necessary calculation, have predicted the present MD results concerning the transverse current. In particular the fact that the second moment becomes very close to zero at large wavevectors.

4. Conclusions.

In this paper, we have presented the molecular dynamics results of dynamical correlations of liquid sodium. We concentrated on the longitudinal and transverse current correlation functions and for the first time we have evaluated the separate contributions of the "self" and "distinct" terms. We have thoroughly examined the variation of these quantities as a function of the wavevector. The rationale of this analysis comes from the recognition that the self-contribution, of both the longitudinal and transverse currents, is very close to another important dynamical quantity that characterizes the liquid phase, i.e. the autocorrelation function of the single particle velocity. This property, which is exact in the limit of $k \to 0$, continues to be fairly well valid even at larger wavevectors. In fact, the possibility of reconstructing this correlation function by a sum of longitudinal and transverse currents, as proposed by Gaskell and Miller [11], allows a more direct insight into their dynamical behavior. In particular, such a result appears to be very illuminating when one examines the longitudinal and transverse spectra separated in terms of self and distinct contributions. The present results show that large cancellations due to the distinct contributions occur both in the longitudinal and transverse spectra in the frequency regions around the main peak and furthermore allow labelling the nature of the remaining intensity. These findings shed new light

18

onto the largely debated question about the possible appearance of quasi-transverse modes in the dynamical structure factor and the corresponding longitudinal current. The analysis of the longitudinal current spectra in terms of self and distinct contributions, has demonstrated that what remains after the large cancellation at small frequencies, is largely due to transverse component of the *self-part*.

The physical interpretation of the distinct term turns out not to be so evident when a comparison is performed between the longitudinal and transverse correlation functions. In particular, the short time behavior is easily interpreted in terms of "momentum transfer" for the transverse correlation since it appears to increase from its value at *t=0*, which by definition is exactly equal to zero, in the whole range of wavevectors examined. On the contrary, for the longitudinal currents it starts to diminish becoming negative at the wavevector $k \approx 0.6$ Å^{-1}, a result that invalidates the interpretation in terms of momentum transfer process. The comparison of our molecular dynamics results, regarding the short time dynamics of these distinct contributions with the theoretical estimates, points out that the validity of our results comes out from the recognition that position and velocity of a particle are strictly correlated when the same Cartesian components are taken into account as done in the longitudinal currents.

19

References.

1. E, Burkel, Inelastic scattering of X-Ray with very high energy resolution, (Springer Verlag, Berlin) 1991.

2. A. Orecchini, W.C. Pilgrim, C.Petrillo, J.B.Suck, F. Sacchetti, Condensed Matter Physics, **11**, 19 (2008)

3. H. Sinn, F. Sette, U. Bergmann, Ch. Halcoussis, M. Krisch, R. Verbeni, , Physical Review Letters **78**, 1715 (1997),

   T. Scopigno, U. Balucani, A. Cunsolo, C. Masciovecchio, G. Ruocco, F. Sette, Europhysics Letters **50**, 189 (2000),

   T. Scopigno, U. Balucani, G. Ruocco, F. Sette, J. of Phys.: Condensed Matter **12**, 8009, (2000),

   T. Scopigno, U. Balucani, G. Ruocco, F. Sette, Physical Review E **65**, 031205 (2002),

   T. Scopigno, G. Ruocco, and F. Sette, Rev. Mod. Phys. **77**, 881 (2005).

4. T. Scopigno, U. Balucani, G. Ruocco, F. Sette, Physical Review E **63**, 011210 (2000),

   T. Scopigno, A. Filipponi, M. Krisch, G. Monaco, G. Ruocco, and F. Sette, Physical Review Letters, **89**, 255506 (2002),

   S. Hosokawa, M. Inui, Y. Kajihara, K. Matsuda, T. Ichitsubo,W.-C. Pilgrim, H. Sinn, L. E. Gonzalez, D. J. Gonzalez, S. Tsutsui, and A. Q. R. Baron, Phys. Rev. Lett. **102**, 105502 (2009).

   S. Sengul, D. J. Gonzalez, and L. E. Gonzalez, J. Phys.: Condens. Matter **21**, 115106 (2009).

   J. Souto, M. M. G. Alemany, L. J. Gallego, L. E. Gonzalez, and D. J.Gonzalez, Phys. Rev. B **81**, 134201 (2010).

   V. M. Giordano and G. Monaco Phys. Rev. B **84**, 052201, 2011

   S. Munejiri, F. Shimojo, and K. Hoshino, Phys. Rev. B **86**, 104202 (2012).

   S. Hosokawa, S. Munejiri, M. Inui, Y. Kajihara, W.-C. Pilgrim, Y. Ohmasa, S. Tsutsui, A. Q. R. Baron, F. Shimojo, and K. Hoshino, J. Phys.: Condens. Matter **25**, 112101 (2013).

E. Guarini, U. Bafile, F. Barocchi, A. De Francesco, E. Farhi, F. Formisano, A. Laloni, A. Orecchini, A. Polidori, M. Puglini, and F. Sacchetti, Phys. Rev. B **88**, 104201 (2013)

R. M. Khusnutdinoff and A. V. Mokshin, JETP Lett. 100, 39 (2014).

S. Hosokawa, M. Inui, Y. Kajihara, S. Tsutsui, and A. Q. R. Baron, J. Phys.:Condens. Matter **27**, 194104 (2015).

M. Zanatta, F. Sacchetti, E. Guarini, A. Orecchini, A. Paciaroni, L. Sani, and C. Petrillo, Phys. Rev. Lett. **114**, 187801 (2015).

M. Inui, Y. Kajihara, S. Munejiri, S. Hosokawa, A. Chiba, K. Ohara, S.Tsutsui, and A. Q. R. Baron, Phys. Rev. B **92**, 054206 (2015).

5. U. Balucani, M. Zoppi, *"Dynamics of the liquid state"* (Clarendon Press Oxford, 1994).

6. V.M. Giordano and G. Monaco, Proc. Natl. Acad. Sci. U. S. A. **107**, 21985 (2010).

7. G. De Lorenzi-Venneri and R. Vallauri, arXiv:1509.03255v [cond-mat.soft] 10 Sept. 2015.

8. U.Balucani, A. Torcini and R. Vallauri, Phys. Rev. B **47**, 3011,(1993)

9. D.L. Price, K. S. Singwi and M. P. Tosi, Physical Review B **2,** 2983, (1970).

10. U. Balucani, R. Vallauri, C.S. Murthy, T. Gaskell and M.S. Woolfson, J. Phys. C: Solid State Phys. **16**, 5605 (1983).

11. T. Gaskell and S. J. Miller, Phys. C: Solid State Phys. **11**, 3749 and 4839 (1978).

12. J.R.D. Copley and S.W. Lovesey Rep. Prog. Phys. **38**, 461 (1975).

13. H. Mori, Prog. Theor. Phys. **33** 423, (1965); R. Zwanzig, Lectures in Theoretical Physics, Boulder vol. 111, ed. W E Britton, B W Downs and J Downs (New York: Interscience) (1961).

14. T. Gaskell and S. F. Duffy, J. Phys.; Condensed Matter, **11**, 6203 (1989).

longitudinal

transverse

correlation functions

time (ps)

time (ps)

full